Smart Test Strips: Next-Generation Inkjet-Printed Wireless Comprehensive Liquid Sensing Platforms

Wenjing Su, *Student Member*, *IEEE*, and Manos M. Tentzeris, *Fellow*, *IEEE*

***Abstract*—By combining radio-frequency identification (RFID) and paper-microfluidics technologies, a low-cost first-of-its-kind platform for comprehensive liquid sensing, the "smart test strip", is presented, which enables portable wireless real-time liquid sensing with handhold devices (e.g. cell phones), and integration of various multifunctional electrical and chemical sensors, for numerous Lab-On-Chip (LOC) applications including manufacturing control, environmental monitoring, and point-of-care medical diagnostic. The fabrication of RFID tags and two types of microfluidics are accomplished by a single inkjet-printing process in a cost-effective environmental-friendly additive manufacturing approach, which makes possible the production of disposable, light-weight and flexible sensing platforms. Taking advantage of the proposed smart test strips platforms, we demonstrate two proof-of-concept high-performance electrical sensors based on Interdigitated Electrode (IDE) topologies: a resistivity-based sensor with a 1782 Ω/(Ω*m) sensitivity; nevertheless, the proposed permittivity-based sensor with a 15%/ϵ_r sensitivity, but the proposed integrated wireless platform can facilitate the integration of even more chemical and electrical sensors. Plus, two on-strip antenna prototypes have been designed, optimized and tested to work at 2.4 GHz and 13.56 MHz, respectively. Furthermore, the wireless interrogation of a complete proof-of-concept smart test strip is presented, which shows an excellent sensing resolution of 1.33 Ω over the range of 0-1371 Ω.**

***Index Terms*—Additive manufacturing, health monitoring, inkjet-printing, Lab on Chip, liquid sensing, microfluidics, paper, RFID, sensors, μPAD, wireless sensing**

I. Introduction

TEST strips are widely used in chemical and biomedical assays in virtually every scenario from industrial manufacturing control to personal healthcare, as they are typically disposable, lightweight and easy to use. In order to enhance the functionality of test strips, in 2007, Whitesides and colleagues developed paper-microfluidics [1]. They patterned the channel and divided the paper into different functional areas, by printing hydrophobic walls on paper. Since then, paper-microfluidics and paper-based microfluidic analytical devices (uPAD) have been in spotlight as they enable the integration of multiple chemical tests into a single strip [2]–[4] at a very low cost due to the additive manufacturing methods used [5], [6]. The more sensors the sensing platform includes, the more effective and comprehensive information about the tested liquid the tester can learn. It is natural to investigate whether it would be possible to integrate more sensors in a cost-effective way within these small test strips.

Recently, the number of electrical and electrochemical liquid sensors has grown significantly, as these sensors can easily turn the liquid information into electrical signals, which can be easily transmitted and recorded [7], [8]. Of special interest are the permittivity and conductivity values of the liquid under test, which effectively disclose contents' information. For example, fat content in milk [9] and fermentation of wines [10] can be easily monitored by the permittivity value, while the contamination of ground water can be detected by an abnormal conductivity value [11]. By embedding the microfluidic channel into the electrical circuits, various microfluidics sensors have been developed to enable real-time monitoring [8], [12], [13]. Combining passive Radio-frequency identification (RFID) technologies, the sensing information obtained from microfluidics sensors can be sent out wirelessly while eliminating the need for power / batteries [14], [15]. Simply, a small RFID chip and an antenna can constitute a well-functioning passive RFID tag commonly used in tracking, locating and recently sensing applications. This light-weight low-cost and compact approach happen to be in the same route as μPAD, so it is natural to combine these two technologies to build a new generation of wireless comprehensive sensors - the smart test strips.

In this paper, we propose the integration of paper-microfluidics chemical sensors and RFID-enabled wireless electrical sensors for comprehensive liquid sensing for the first time. On one side, regular paper-microfluidics chemical sensors usually use a specific chemical reagent in each sensor to detect a specific content, such as glucose or protein [2]–[4]. On the other side, electrical sensors sense liquid's information, such as conductivity or permittivity which is a composite result of all liquid's contents [8], [12], [13]. The smart test strip can obtain information from both (individual/composite), which allows for more degrees of monitoring, increases the information capacity, and significantly saves tester's time and effort.

Manuscript received November 21, 2016; revised February 16, 2017 and March 26, 2017; accepted April 18, 2017. This work was supported in part by the Office of Emerging Frontiers and Multidisciplinary Activities of National Science Foundation (NSF-EFRI), Defense Threat Reduction Agency (DTRA), Semiconductor Research Corporation (SRC).

W. Su and M. M. Tentzeris are with the School of Electrical and Computer Engineering, Georgia Institute of Technology, Atlanta, GA 30332-250, USA (e-mail: wenjing.su.gatech@gmail.com, etentze@ece.gatech.edu).

This article has been accepted for publication in a future issue of this journal, but has not been fully edited. Content may change prior to final publication. Citation information: DOI 10.1109/TIE.2017.2708022, IEEE Transactions on Industrial Electronics

Compared with traditional sensors or sensing platforms, the proposed systems can provide comprehensive information in a wireless and portable approach, which improves the efficiency drastically and enables next-generation liquid sensing.

In order to realize ubiquitous sensing and deploy the proposed smart test strips in massive scale, the strips including both the microfluidics and the RFID tags, must be fabricated in a consistent and cost-efficient way. Inkjet-printing, a low-cost environmental-friendly additive manufacturing (AM) technique, has been introduced in RFID fabrication [16], [17], while also being capable of effectively realizing microfluidics [8], [15], [18]. Inkjet-printing, one of the most common techniques used in commercial printing industry, is a scalable process, which means the fabrication time doesn't increase largely with the increase of samples' quantity and thus is good for high volume industrial production. In this work, fully inkjet-printed microfluidics, fully inkjet-printed μPAD and fully inkjet-printed RFID tags are realized in the same platform to achieve a cost- and time-efficient fabrication of the smart test strip. To the best of authors' knowledge, inkjet-printing is the only tool that can facilitate the fabrication of all these three parts easily and cost-effectively, so it is one of the best candidates for the fabrication of the smart test strips. Compared with fabricating these three parts separately and assembling afterwards, the proposed fully inkjet-printing process can effectively eliminate the equipment cost, while saving time and space of assembly. Therefore, we present the smart strip sensing platform along with a low-cost fabrication approach, featuring disposable, light-weight, zero-power, multi-functional, time-and-effort-efficient characteristics and wide applicability to numerous scenaria including water quality monitoring, manufacturing control, and point of care medical diagnostic.

This paper is arranged in the following way: section II provides a system-level overview of the wireless smart test strips; section III discusses the challenges and solutions for the low-cost easy-to-scale fabrication of the proposed smart test strips; two types of electrical sensors along with their proof-of-concept prototypes on the test strips are presented in section IV; section V discusses the wireless interrogation of the electrical sensing platforms on the smart test strips.

II. System Overview

The proposed smart test strips system consists of various smart strips and one reader as shown in Fig. II. Within every individual test strip, there are multiple chemical sensors, such as pH, glucose and protein, which are divided in different sections and deposited with different reagents that react with the testing content and produce colorful compounds. Based on the color intensity, the concentration of the chemical content under test can be detected. Various researchers in chemical and biomedical area have reported numerous sensors of this type [1]–[3]. In addition to the chemical sensors, multiple electrical sensors, such as permittivity sensors, conductivity sensors, and temperature sensors, are also embedded within the test strips taking advantage of their inherent property to easily translate the liquid's information to a resistance or capacitance change.

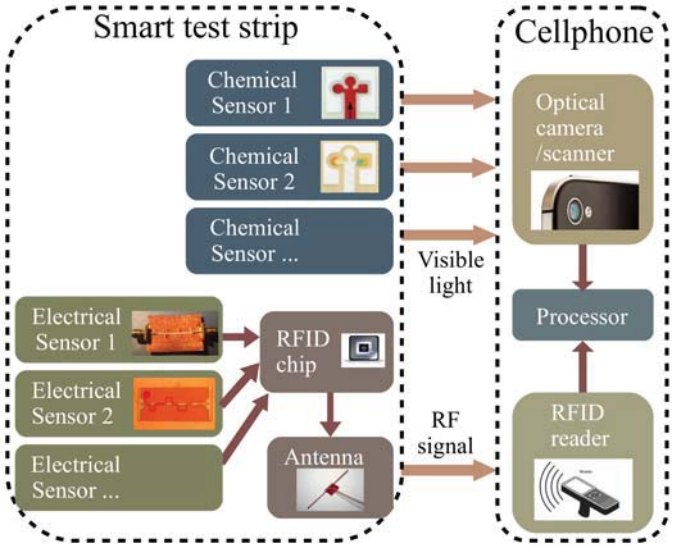

Fig. 1. A block diagram of the proposed smart test strips system-level operation principle.

The RFID chip then digitizes the resistance or capacitance to a binary signal, which is afterwards transmitted back through the antenna to the reader/gateway employing backscattering techniques. The chemical sensors obtain information about specific and/or expected chemical substances within the liquid under test, while the electrical sensors provide the comprehensive overall status including the composite effect of all contents.

A proof-of-concept prototype of the proposed smart test strip platform with two electrical sensors, three chemical sensors, and an antenna, is shown in Fig. 2a and another realization of the same system topology including an electrical sensor, a chemical sensor and an antenna operating in lower frequencies is shown in Fig. 8b. The smart test strip can also be realized on off-the-shelf chemical sensors such as the PH strip shown in Fig. 3a, with the cross-section view of the microfluidic channels shown in Fig. 3b When a drop of liquid reaches the opening of the stand-alone channel, the channel would imbibe the liquid because of the capillary effect. Afterwards, the liquid goes through the electrical sensors inside the stand-alone channel and then comes to the paper-microfluidics to interact with the chemical reagents.

On the reader side, portable devices, such as cell phones, can perform the reading easily: the phone cameras can be used to digitize the intensity of color of each chemical sensor [19]; the antenna on the phone is capable to transmit and receive the RFID backscattering signal in the meantime. The phone can then send it to an off-site laboratory for analysis by a trained professional or immediately filter it through preset criteria in the phone and directly return the testing conclusions.

III. Fabrication

As inexpensiveness, scalability and disposability are key requirements to ensure the ubiquitousness of the proposed smart test strips, additive manufacturing techniques with adequate

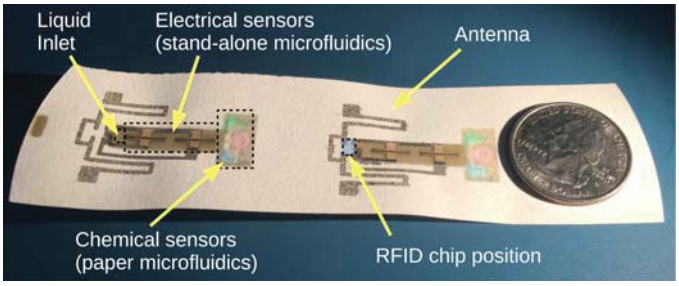

(a)

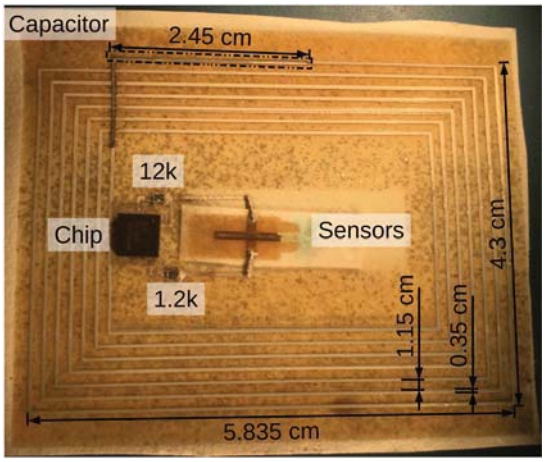

(b)

Fig. 2. A photo of fabricated smart test strip prototypes working at (a) wireless and (b) Near-Field communication frequencies.

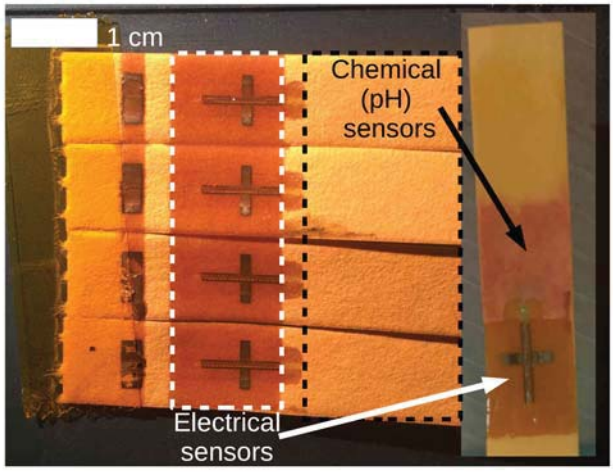

(a)

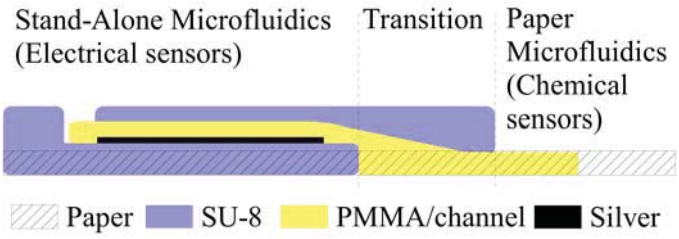

(b)

Fig. 3. (a) A photo of multiple smart electrical sensors integrated on pH test strips along with an inserted photo (right) of one pH smart strip tested by vinegar confirming the unaffected good performance of the chemical sensor. (b) A drawing of the cross-section view of the smart test strip channel topology.

resolution, such as inkjet-printing, would be among the best fabrication solutions.

A. Inkjet-printing configuration

For the fabrication of the proof-of-concept prototypes, inkjet-printing was conducted by a high-performance Dimatix DMP-2831 materials deposition printer (Fujifilm Dimatix, Inc., Santa Clara, USA) with a 10 pL drop volume of a 16-nozzle cartridge (DMC-11610, Fujifilm Dimatix, Inc.). The print heads of the printer facilitate depositing inks with a viscosity in the range of 8 to 12 cP, and a surface tension in the range of 20 to 30 mN/m. The two substrates tested in this paper are Whatman filter paper and Lab supplies universal indicator PH test strip, although any filter paper or test strip is expected to feature a similar performance. The three inks involved in inkjet-printing were Sun Chemical Suntronic silver nanoparticle (SNP) ink (Parsippany, USA); SU-8 ink, which is a blend of Microchem SU-8 2002 and SU-8 2005 (Westborough, USA) [20]; PMMA ink, which was realized by dissolving PMMA powder into a mixture of anisole and dimethyl sulfoxide (DMSO) (Sigma-Aldrich Corporation, St. Louis, USA) [18]. The printing time for the whole process is less than 15 minutes in optimal printing conditions and the time for curing/sintering is shown in Table I, which is around 2 hours in total.

TABLE I
INKS AND PRINTING /CURING CONDITIONS

Inks	Printing temperature	Curing condition
SNP	60°C	120°C for 1 hours
SU-8	25°C	Following the data sheet [21]
PMMA	25°C	120°C for 30 mins

B. Electronics

Inkjet-printing has been already extensively utilized in fabricating electronics such as antennas and passive elements [22], [23]. By inkjet-printing conductive nanoparticles, conductive traces which typically enable electrical sensing can be easily fabricated. However, printing on porous substrates, such as paper, can be challenging as the ink will flow into the substrate, instead of remaining on the top of it [24]. In Fig. 4b and 4d, ink deposited on one side can be clearly seen from the other side and spreads out randomly along the paper fibers, which limits the resolution of the printing. Printing conductive nanoparticles can be even more troublesome as they may be separated by paper fibers during sintering, which leads to a decrease in the conductivity. In Fig. 4e, the sheet resistance of the directly printed conductive traces on filter paper / PH strip is over 10 times larger than those printed on smooth non-porous surfaces.

There are two ways to resolve this issue. The “passive” way involves the deposition of an increasing number of layers

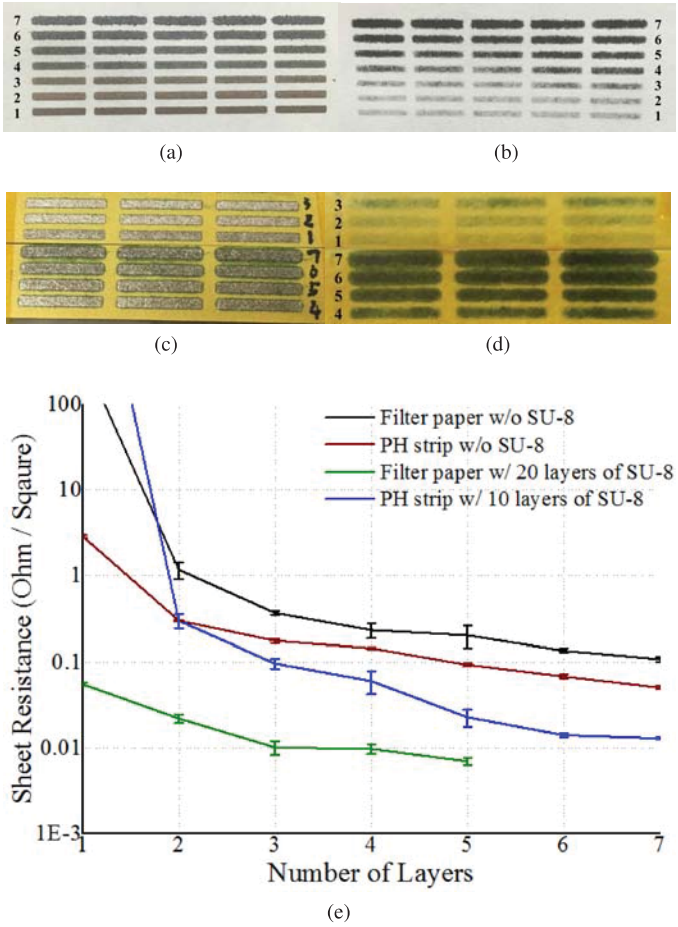

Fig. 4. Inkjet-printed conductive layers on paper. (a, b, c, d) Photos of front (ink deposited side) (a, c) and back (b, d) of different number of layers of silver traces printed on the filter paper (a, b) and PH strip (c, d). (e) Average measured sheet resistance for different number of layers of silver printed on filter papers and PH strips with and without printed SU-8 isolation layers, along with the error bars showing the standard deviations of 20 replicas that were measured 10 times each.

until the saturation of the substrate so that any additional ink will start accumulating on the top of the paper. In Fig. 4e, an acceptable sheet resistance of 0.1 Ω/square is achieved when more than 7 / 5 layers of ink have been deposited on filter paper / PH strip, respectively. The "active" way involves the inkjet-printing of a thick layer of SU-8, which will fill the porous space and form a smooth surface, followed by the inkjet-printing of a silver nanoparticle ink on top of the SU-8, resulting in a much better resolution compared to direct printing on paper. A very high conductivity (0.01 Ω/square sheet resistance) can be reached with only 3 layers of silver nanoparticles ink with sufficient SU-8 deposited and cured first, which is comparable to the case of regular smooth non-porous substrates.

In Fig. 2a, the sensors were printed on SU-8 to maximize the printing resolution while the antenna and routing were printed directly on the filter paper to simplify the process, while in Fig. 2b, all conductive parts were printed on 20 layers of SU-8 to achieve the best resolution.

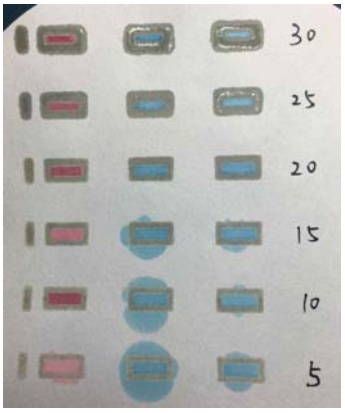

Fig. 5. Different numbers of inkjet-printed layers of SU-8 rectangular rings for paper-microfluidics. The leftmost column was tested with red-dyed water drops and the other two columns were tested with blue-dyed ethanol drops. Water leakage occurred for 5 layers of printed SU-8, while ethanol leakage occurred in the case of less than 20 layers printed.

C. Microfluidics

As shown in Fig. 3b, there are two different microfluidics in this work: paper-microfluidics, which use paper as a propagation medium ("in-the-paper") and only have two sidewalls to constrain the liquid, and stand-alone microfluidics, in which the channel is on top of the substrate ("on-the-paper") and is fully sealed in all four directions. For paper-microfluidics, wax printing is one of the most common fabrication methods [5]. As an alternative, other hydrophobic materials such as SU-8, have been deposited and patterned by photo-lithography to fabricate paper-microfluidics [19]. Here, we propose inkjet-printing SU-8 to fabricate the paper-microfluidics, an approach that features much lower cost than the photo-lithography method and a better resolution compared to wax printing. Furthermore, not "in-the-paper" but "on-the-paper" stand-alone microfluidics can be easily fabricated by inkjet-printing, which feature a better control of the volume of liquid inside the channel that plays a very significant role in electrical sensing. Recently, researchers have used inkjet-printing as a bonding method or as a mode fabrication method to fabricate microfluidics [8], [13]. Moreover, fully inkjet-printing stand-alone microfluidics has been reported [18], which is a low-cost and rapid fabrication approach. Thus, we adapt the inkjet-printing method in this work to fabricate stand-alone microfluidics structure on porous substrates, such as filter paper.

In the smart test strips introduced in this paper, there are three parts in microfluidics as shown in Fig. 3b:

1) Paper-microfluidics: For the first time, paper-microfluidics using patterned SU-8 as the hydrophobic walls on filter paper. Fig. 5 shows the liquid-proof performance for different numbers of printed SU-8 layers demonstrating that 10 layers of SU-8 are sufficient for water while 20 layers are needed for ethanol.
2) Stand-alone microfluidics: fully inkjet-printed stand-alone microfluidics reported in [18] were adjusted for paper substrate. 15 layers of SU-8 were printed to isolate the stand-alone microfluidics from the paper, followed by 10

layers (about 45 μm) of PMMA printed as a support material to effectively define the channel position and configuration. Then, an additional 15 layers (about 90 μm) of SU-8 were printed on top and cured, with the fabrication finalized by the PMMA being washed out by anisole bath.

3) Transition between the two types of microfluidics: By printing a 2-mm-length PMMA trace directly on paper and a 1-mm-length SU-8 layer to partially cover the PMMA trace, as shown in Fig. 3b, the opening of the channel would be in contact with paper and due to the liquid nature of the ink, a nice and smooth slope would be formed automatically over the step, which efficiently leads the flowing liquid to the paper while not blocking the fluid into paper-microfluidics. In order to have a smooth transition between the paper-microfluidics channel and the stand-alone microfluidics channel, the PMMA configuration was chosen to be consistent with the stand-alone channels, while the SU-8 configuration was similar to the one used in the paper-microfluidics structures.

IV. Sensor on Strip

Microfluidics-based electrical sensors have been developed for different applications, such as temperature sensing [8], heavy-metal ion monitoring [25], and glucose concentration detection [26]. Most of them take advantage of the permittivity or conductivity of different liquids by comparing either the current-voltage (I-V) curves or the frequency responses.

A. IDE structures

Fig. 6a shows an electrical sensor on a smart test strip that can enable multiple sensing functions. Interdigitated electrodes (IDEs) were used in this prototype as they effectively increase the surface (sensing) area of the electrodes without increasing the total sensor area. The microfluidic channel is placed right on the top of the IDEs to maximize the sensitivity.

The equivalent circuit of the IDE structure is shown in Fig. 6c; the measured impedance can be approximated by a parallel RC circuit. On the one hand, the total resistance (R_{total}) can be modelled as two resistors in parallel: a constant resistor (R_0) due to the filter paper and a varying resistor (R) due to the liquid inside the channel. Thus, the relation between the varying resistivity (ρ) and the measured/sensed resistance (R_{total}) can be seen in

$$R_{total} = \frac{1}{\frac{1}{R} + \frac{1}{R_0}} \approx R = \frac{d_{eff}}{A_{eff}} \times \rho. \quad (1)$$

Where d_{eff} and A_{eff} are the effective distance and cross-section surface area between the two gap-separated inter-digitated electrodes, while ρ is the resistivity value of the liquid in the channel. In most cases, R_0 is very large, so the approximation in (1) is valid and the measured resistance (R_{total}) is linearly proportional to the resistivity (ρ) of the liquid inside the channel. On the other hand, similarly, the total capacitance (C_{total}) can be calculated through the parallel combination of two capacitors: a constant capacitor (C_0) due to the filter paper and a varying capacitor (C) due to the liquid inside the channel. The relation between the varying

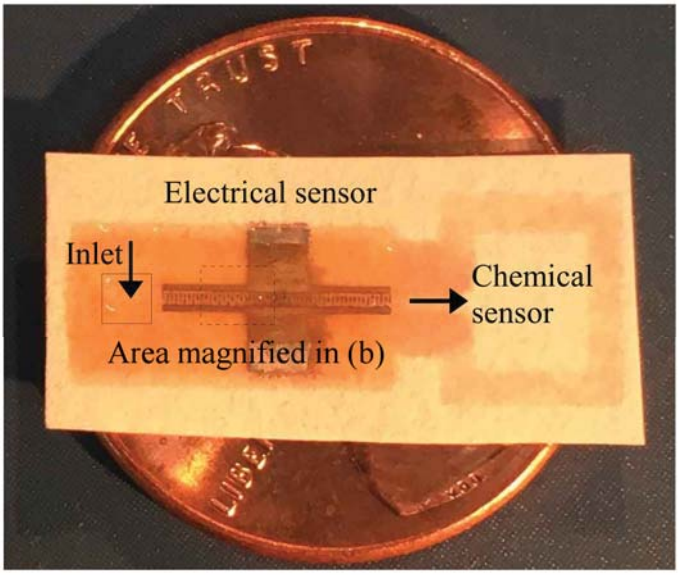

(a)

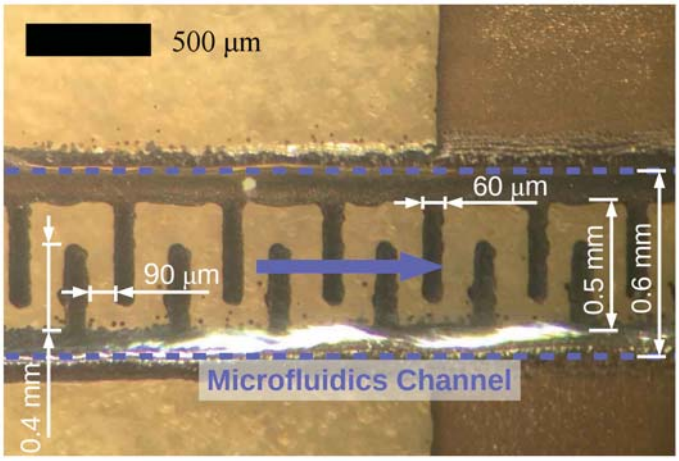

(b)

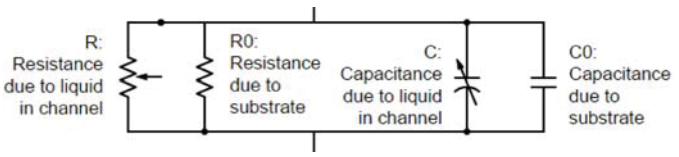

(c)

Fig. 6. (a) A photo of a printed sensor prototype compared to an 1-cent coin. (b) Magnified view of the interdigitated electrode (IDE) structure in the dashed square in (a). (c) Equivalent circuit of the IDE sensors.

permittivity (ϵ_r) and the detected capacitance (C_{total}) can be calculated applying the parallel-plate capacitor model and is given by

$$C_{total} = C + C_0 \approx \frac{A_{eff} \times \epsilon_0}{d_{eff}} \times \epsilon_r + C_0. \quad (2)$$

ϵ_r is the relative permittivity of the tested liquid, while ϵ_0 is the free space permittivity. With the approximation in (2), the measured/sensed composite capacitance (C_{total}) is linearly proportional to the relative permittivity (ϵ_r) inside the channel.

To simplify the real-time measurements and avoid dealing with complex impedances, the IDE structure can be treated

TABLE II
CONDUCTIVITY OF DIFFERENT SODIUM CHLORIDE (NACL) AQUEOUS SOLUTIONS FOR VARIOUS CONCENTRATIONS [27]

Concentration (Mol/L)	Conductivity (S/m)
0.0	5.5e-6
0.10	1.2
0.35	3.7
1.0	10
3.5	40

as either a resistor or a capacitor: in the case that the tested liquid has a relatively high conductivity or DC voltage is applied ($R_{total} << \frac{1}{\omega \times C_{total}}$, where ω is the measurement radial frequency), the imaginary part of the impedance can be neglected and the IDE structure can be seen as a simple resistor; otherwise, if the tested liquid is non-conducting and AC voltage is applied, the IDE structure structure can be approximated by a capacitor.

B. Resistivity-based Sensing

Resistivity-based sensors are widely used in electrochemical sensing, especially for ion detection. In water quality testing, resistivity values usually imply the salinity [27], [28], which has a large impact in plants growth and agriculture, as high-salinity water would dehydrate and kill the plants. Moreover, the conductivity of the water is strongly related to the ion concentration. For example, sea water's conductivity is one million times higher than that of deionized water and the conductivity of various aqueous sodium chloride (NaCl) solutions with different concentrations is shown in Table II. Therefore, resistivity-based sensors play an essential role in water quality test kits and are of significance in the smart test strips.

An IDE-based resistivity sensor was simulated by COMSOL Multiphysics modeling software and measured with an Agilent U1733C handhold LCR meter on the probe station with a parallel RLC setting as shown in Fig. 7a. The LCR meter was connected to two probes, which were calibrated with open and short circuits before performing the measurement. The simulated resistance of the sensor (the simulated results were derived from the complex impedance of the equivalent circuit shown in Fig. 6c) vs resistivity of the liquid inside the microfluidic channel is shown in Fig. 7b, along with measurement results for various sensor-filling aqueous solutions of sodium chloride featuring a sensitivity of 1782 Ω/(Ω*m), which is superior compared to subtractively manufactured IDE sensors [29]. The concentration of the sodium chloride in the water can be easily determined from the measurements.

C. Permittivity-based Sensing

The values of permittivity (also called dielectric constant in some cases) of the liquids in the natural environment vary widely, as shown in Table III. Mixtures of two or more fluids can feature a wide range of continuous permittivity as a function of the mixing ratios [31]. Similarly, the permittivity of the solution varies depending on its concentration [27], [32]. Thus, if a device is capable of detecting small changes in the permittivity values of a liquid, it may deduce a significant amount of information about it.

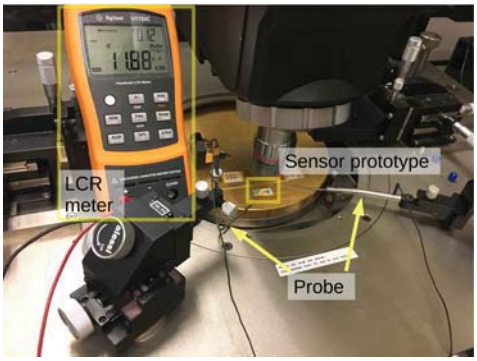

(a)

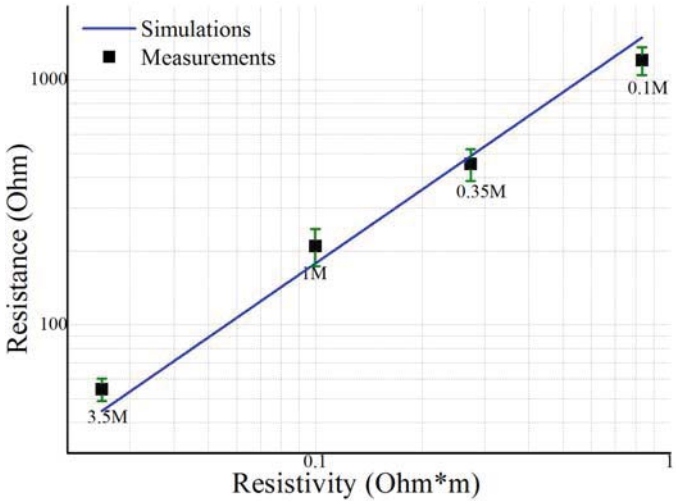

(b)

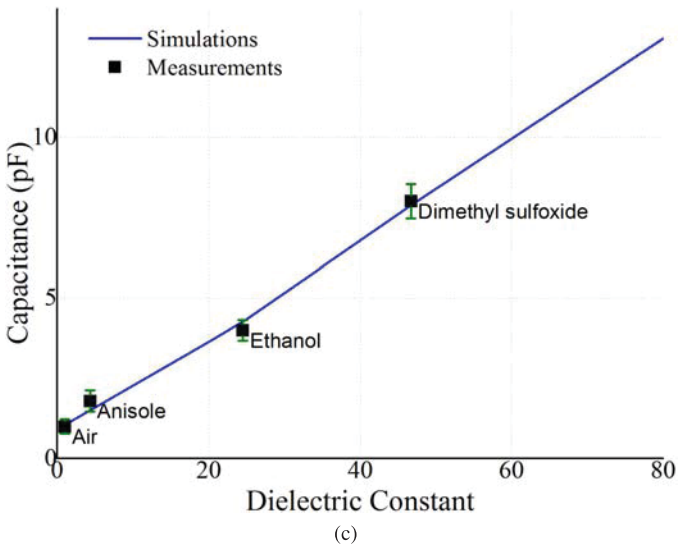

(c)

Fig. 7. (a) Measurement setup for the microfluidic sensor testing. (b) Simulated and measured average resistance of the sensor for filling liquids with different concentration (resistivity), along with the error bars showing the standard deviations of 20 replicas that were measured 10 times each. (c) Simulated and measured average capacitance of the sensor for filling liquids with different dielectric constants, along with the error bars showing the standard deviations of 20 replicas that were measured 10 times each.

TABLE III
DIELECTRIC CONSTANT OF AIR AND THREE ORGANIC FLUIDS AT 1 KHZ AND ROOM TEMPERATURE [30]

Name	Dielectric constant (ϵ_r)
Air	1.00
Anisole	4.33
Ethanol	24.3
Dimethyl sulfoxide	46.7
Deionized water	80.0

Similar to the resistance-based sensing, the relationship between the measured capacitance and the liquid's permittivity was simulated by the COMSOL modeling software and measured with the LCR meter at 1 kHz with the results displayed in Fig. 7c. The sensor prototype was characterized for 4 different materials (air and three organic fluids) filling the microfluidic channel with the respective dielectric constants shown in Table III, featuring an excellent sensitivity of $15\%/\epsilon_r$ (or 0.15 pF/ϵ_r), which enables the sensing of very small liquid content changes and is superior compared to subtractively manufactured IDE sensors [29], [33]. For example, the permittivity of ethanol and water mixtures is varying by 5.5 for every 10% weight mixing ratio difference at room temperature, according to [34]. Therefore, if the prototyped sensor is used in alcohol/wine testing, the sensitivity would be 8.25%/wt.%, which means 1% of mixing ratio changes will lead to 8.25% capacitance variation, given that the measured sensitivity is $15\%/\epsilon_r$.

V. WIRELESS INTERROGATION

RFID technologies could potentially revolutionize the efficient wireless interrogation of the proposed smart strip sensors. As the smart test strips are designed to work with portable devices, such as cell phones, that read the RFID while scanning the color of a chemical sensor at the same time, a small reader range ($<$ 20 cm) would be required, which fits very well with the use of passive RFID's, that can be waken up / interrogated with very low power levels while eliminating the need for batteries. Recently, new RFID sensor chips enabling the Internet of Things (IoT) were invented at both academia [35], [36] and industry, while new RFID chips at HF and UHF band that have multiple external pads for resistivity reading have been on the market, such as Melexis MLX90129, TI RF430FRL, or AMS SL13A and SL900A. With the help of those chips, the capacitance and resistance sensing values can be easily converted to binary code and sent to the reader through the use of antennas. Typical smart test strip configurations allow for the easy and direct integration of the antennas on the filter paper, which largely simplifies the process and decreases the resulting cost.

A. Filter paper electrical characterization

In order to successfully design antennas on the strip, the material properties of the filter paper were characterized up to the wireless frequency ranges with the T-resonator method [37] and the two transmission lines method [38]. The results showed that the permittivity of the paper is 1.73 and the loss tangent was calculated to be 0.036 at 2.4 GHz. Both values are clearly low compared to other paper types (e.g. photo papers) characterized over the same frequencies [17], [39] that feature permittivity values above 3 and loss tangent values above 0.06, which is very likely due to air filling in the porous structure of the filter paper.

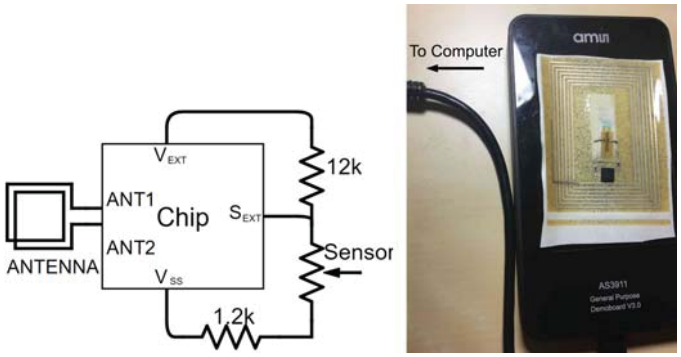

(a) (b)

Fig. 8. (a) The schematic of the external circuit to the RFID chip. (b) A photo of the measurement setup of a smart test strip with an NFC RFID reader.

B. Wireless System Realization and Testing

For proof-of-concept purposes, a smart test strip was designed with a coil antenna working at 13.56 MHz, an AMS SL13A RFID chip, two resistors and a resistivity sensor, as shown in the Fig. 2b. 13.56 MHz wireless configurations were chosen due to the widely-available off-the-shelf RFID / Near Field Communication (NFC) chips and due to many existing phones being equipped with the NFC capability for applications such as mobile payments. The schematic of the external circuit connected to the chip is shown in Fig. 8a. A coil antenna with a capacitive structure at the end was designed with Ansoft HFSS to resonate at 13.56 MHz. The coil in Fig. 2b features a size similar to credit cards, while in space-constrained scenaria, more miniaturized antennas operating in higher frequencies can be used, as discussed in Section V.C. By harvesting RF power from the reader, the chip can supply 3.4-V output voltage (at V_{EXT}) to the sensor circuit. The ADC circuit in the chip (at S_{EXT}) can convert voltage values between 300 mV and 600 mV to 10-bits digits, therefore two resistors (12 kΩ and 1.2 kΩ, respectively) were used to divide the output power appropriately to the sensor. Fig. 8b shows the measurement setup for the wireless interrogation of the test strip. The strip was read by an AMS AS3911 general purpose NFC reader in a 1-cm distance and the connected computer decoded the NFC signals into a unitless numeric sensing readout from -100 to 60 as shown in Fig. 9. Firstly, various voltages were applied to S_{EXT} and respective readings were recorded to calculate the curve in Fig. 9, which demonstrates the performance of the RFID tag platform. Then the IDE-based resistivity sensor was added and sodium chloride aqueous solutions with four different concentrations were filled to test the performance of the integrated system. For the above

This article has been accepted for publication in a future issue of this journal, but has not been fully edited. Content may change prior to final publication. Citation information: DOI 10.1109/TIE.2017.2708022, IEEE Transactions on Industrial Electronics

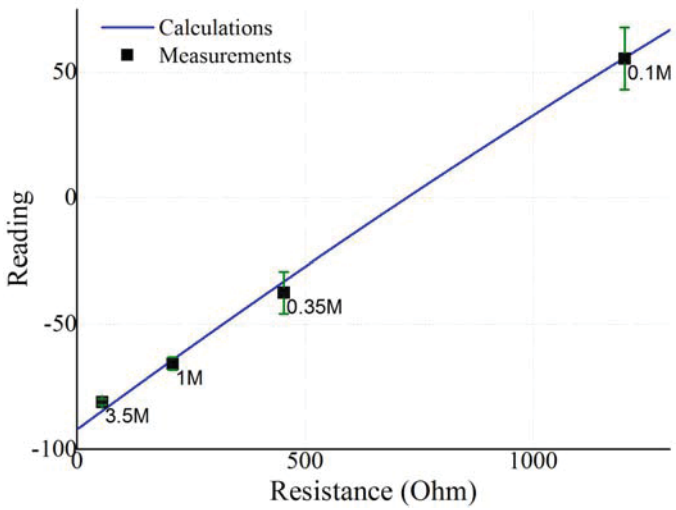

Fig. 9. Calculated wireless reading of the smart test strip prototype in an NFC chip configuration along with measured values for sodium chloride aqueous solutions of different concentrations, along with the error bars showing the standard deviations of measuring the sample for 20 times.

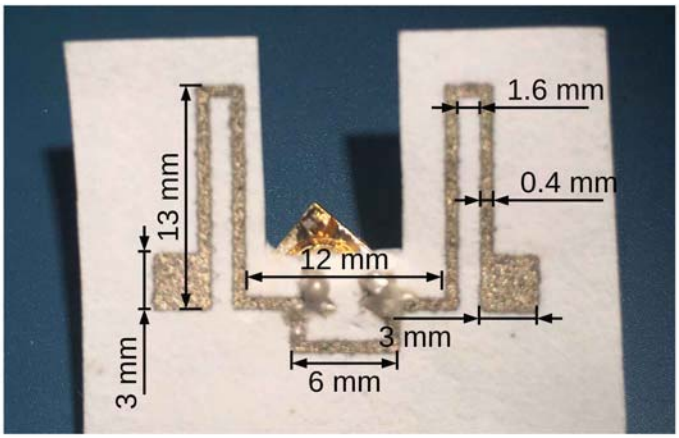

Fig. 10. Inkjet-printed meander-line dipole antenna on filter paper for wireless smart test strips.

mentioned configuration, the sensor can sense the resistance change of the sensor from 0 to 1300 Ω, with an average minimal detectable resistance change (sensing resolution) of 1.33 Ω, demonstrating an excellent wireless sensing capability of the smart test strip.

C. Extension to Wireless Frequencies

Wireless frequencies, e.g. 2.4 GHz, feature a great potential for the smart test strip, as they have excellent compatibility with existing cell phone antennas as well as a better compactness compared to NFC frequencies. However, limited choices of off-the-shelf RFID sensor chips operating at 2.4 GHz were observed. Here, an inkjet-printed tag antenna on filter paper operating around 2.4GHz is presented to demonstrate the potential of operating the smart test strips at wireless frequencies. A meander line dipole antenna, as shown in Fig. 10, was designed due to its inherent miniaturization properties thus enhancing flexibility and wearability. The antenna was simulated by a full-wave simulator (Ansoft HFSS) and was

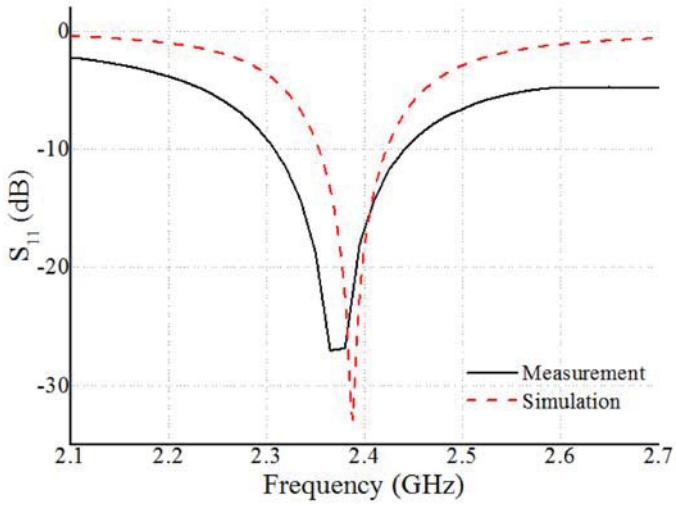

Fig. 11. Simulated and measured return loss (S11) of the inkjet-printed dipole antenna on filter paper.

measured by a Rhode and Schwartz ZVA-8 Vector Network Analyzer (VNA) with results shown in Fig. 11. A good impedance matching with a maximum gain of 1.3 dBi was observed, which is comparable to other inkjet-printed antennas on paper substrates [17] and verifies the feasibility of smart test strips operating at wireless frequencies.

VI. Conclusion

A novel low-cost wireless platform ("smart test strip") for comprehensive next-generation liquid sensing is presented in this paper by combining uPAD (paper-microfluidics) and RFID technologies. The fabrication of RFID tags and two types of microfluidics are accomplished by inkjet-printing, a low-cost additive manufacturing method, which allows for a disposable, lightweight, flexible, scalable, and time-and-effort-efficient fabrication. The proposed platform enables the integration of multiple chemical and electrical sensors, thus multi-functional, highly reliable and comprehensive liquid sensing can be realized. IDE based on inkjet-printed electrical sensors were presented and evaluated with an excellent capability to distinguish sodium chloride solutions of different concentrations and various organic liquids. The dielectric properties of the filter paper were characterized up to the wireless frequencies for the first time (ϵ_r: 1.7, loss tangent: 0.036 at 2.4 GHz). Proof-of-concept RFID/NFC tags at 13.56 MHz and 2.4 GHz were designed and an NFC-based smart test strip was measured with a commercial reader featuring 1.33 Ω average minimal detectable resistance change in the range from 0 to 1300 Ω. The proposed smart test strips could find numerous applications, that would include, among others, manufacturing control, water quality monitoring, and point-of-care medical diagnostics.

References

[1] A. W. Martinez, S. T. Phillips, M. J. Butte, and G. M. Whitesides, "Patterned paper as a platform for inexpensive, low-volume, portable bioassays," *Angewandte Chemie International Edition*, vol. 46, no. 8, pp. 1318–1320, 2007.

[2] K. Abe, K. Suzuki, and D. Citterio, "Inkjet-printed microfluidic multianalyte chemical sensing paper," *Analytical chemistry*, vol. 80, no. 18, pp. 6928–6934, 2008.

[3] A. K. Yetisen, M. S. Akram, and C. R. Lowe, "Paper-based microfluidic point-of-care diagnostic devices," *Lab on a Chip*, vol. 13, no. 12, pp. 2210–2251, 2013.

[4] Y. Yang, E. Noviana, M. P. Nguyen, B. J. Geiss, D. S. Dandy, and C. S. Henry, "Paper-based microfluidic devices: Emerging themes and applications," *Analytical Chemistry*, 2016.

[5] E. Carrilho, A. W. Martinez, and G. M. Whitesides, "Understanding wax printing: a simple micropatterning process for paper-based microfluidics," *Analytical chemistry*, vol. 81, no. 16, pp. 7091–7095, 2009.

[6] Y. Xia, J. Si, and Z. Li, "Fabrication techniques for microfluidic paper-based analytical devices and their applications for biological testing: A review," *Biosensors and Bioelectronics*, vol. 77, pp. 774–789, 2016.

[7] Z. Nie, C. A. Nijhuis, J. Gong, X. Chen, A. Kumachev, A. W. Martinez, M. Narovlyansky, and G. M. Whitesides, "Electrochemical sensing in paper-based microfluidic devices," *Lab on a Chip*, vol. 10, no. 4, pp. 477–483, 2010.

[8] C. Mariotti, W. Su, B. S. Cook, L. Roselli, and M. M. Tentzeris, "Development of low cost, wireless, inkjet printed microfluidic RF systems and devices for sensing or tunable electronics," *IEEE Sensors Journal*, vol. 15, no. 6, pp. 3156–3163, 2015.

[9] W. Guo, X. Zhu, H. Liu, R. Yue, and S. Wang, "Effects of milk concentration and freshness on microwave dielectric properties," *Journal of Food Engineering*, vol. 99, no. 3, pp. 344–350, 2010.

[10] A. Garcia, J. Torres, M. De Blas, A. De Francisco, and R. Illanes, "Dielectric characteristics of grape juice and wine," *Biosystems engineering*, vol. 88, no. 3, pp. 343–349, 2004.

[11] M. Arshad, J. Cheema, and S. Ahmed, "Determination of lithology and groundwater quality using electrical resistivity survey," *International Journal of Agriculture and Biology*, vol. 9, no. 1, pp. 143–146, 2007.

[12] K. Grenier, D. Dubuc, P.-E. Poleni, M. Kumemura, H. Toshiyoshi, T. Fujii, and H. Fujita, "Integrated broadband microwave and microfluidic sensor dedicated to bioengineering," *IEEE Transactions on microwave theory and techniques*, vol. 57, no. 12, p. 3246, 2009.

[13] W. Su, B. S. Cook, and M. M. Tentzeris, "Additively manufactured microfluidics-based "peel-and-replace" RF sensors for wearable applications," *IEEE Transactions on Microwave Theory and Techniques*, vol. 64, no. 6, pp. 1928–1936, 2016.

[14] R. Want, "Enabling ubiquitous sensing with RFID," *IEEE Computer*, vol. 37, no. 4, pp. 84–86, 2004.

[15] W. Su, Q. Liu, B. Cook, and M. Tentzeris, "All-inkjet-printed microfluidics-based encodable flexible chipless RFID sensors," in *2016 IEEE MTT-S International Microwave Symposium (IMS)*, DOI 10.1109/MWSYM.2016.7540411, May. 2016, pp. 1–4.

[16] S. Molesa, D. R. Redinger, D. C. Huang, and V. Subramanian, "High-quality inkjet-printed multilevel interconnects and inductive components on plastic for ultra-low-cost RFID applications," in *Materials Research Society Symposium Proceedings*, vol. 769. Warrendale, Pa.; Materials Research Society; 1999, 2003, pp. 253–258.

[17] L. Yang, A. Rida, R. Vyas, and M. M. Tentzeris, "RFID tag and rf structures on a paper substrate using inkjet-printing technology," *IEEE Transactions on Microwave Theory and Techniques*, vol. 55, no. 12, pp. 2894–2901, 2007.

[18] W. Su, B. S. Cook, Y. Fang, and M. M. Tentzeris, "Fully inkjet-printed microfluidics: a solution to low-cost rapid three-dimensional microfluidics fabrication with numerous electrical and sensing applications," *Scientific Reports*, vol. 6, p. 35111, 2016.

[19] A. W. Martinez, S. T. Phillips, E. Carrilho, S. W. Thomas III, H. Sindi, and G. M. Whitesides, "Simple telemedicine for developing regions: camera phones and paper-based microfluidic devices for real-time, off-site diagnosis," *Analytical chemistry*, vol. 80, no. 10, pp. 3699–3707, 2008.

[20] B. S. Cook, B. Tehrani, J. R. Cooper, and M. M. Tentzeris, "Multilayer inkjet printing of millimeter-wave proximity-fed patch arrays on flexible substrates," *IEEE Antennas and Wireless Propagation Letters*, vol. 12, pp. 1351–1354, 2013.

[21] *SU-8 2000*, Microchem, www.microchem.com/pdf/SU-82000DataSheet2000_5thru2015Ver4.pdf.

[22] J. Lessing, A. C. Glavan, S. B. Walker, C. Keplinger, J. A. Lewis, and G. M. Whitesides, "Inkjet printing of conductive inks with high lateral resolution on omniphobic "rf paper" for paper-based electronics and mems," *Advanced Materials*, vol. 26, no. 27, pp. 4677–4682, 2014.

[23] J. G. Hester, S. Kim, J. Bito, T. Le, J. Kimionis, D. Revier, C. Saintsing, W. Su, B. Tehrani, A. Traille *et al.*, "Additively manufactured nanotechnology and origami-enabled flexible microwave electronics," *Proc. IEEE*, vol. 103, no. 4, pp. 583–606, 2015.

[24] S. A. Nauroze, J. Hester, W. Su, and M. M. Tentzeris, "Inkjet-printed substrate integrated waveguides (siw) with "drill-less" vias on paper substrates," in *Microwave Symposium (IMS), 2016 IEEE MTT-S International*. IEEE, 2016, pp. 1–4.

[25] M. Li, H. Gou, I. Al-Ogaidi, and N. Wu, "Nanostructured sensors for detection of heavy metals: a review," *ACS Sustainable Chemistry & Engineering*, vol. 1, no. 7, pp. 713–723, 2013.

[26] T. Chretiennot, D. Dubuc, and K. Grenier, "Double stub resonant biosensor for glucose concentrations quantification of multiple aqueous solutions," in *2014 IEEE MTT-S International Microwave Symposium (IMS2014)*. IEEE, 2014, pp. 1–4.

[27] V. G. Artemov, A. A. Volkov, N. N. Sysoev, and A. A. Volkov, "Conductivity of aqueous hcl, naoh and nacl solutions: Is water just a substrate?" *EPL (Europhysics Letters)*, vol. 109, no. 2, p. 26002, 2015. [Online]. Available: http://stacks.iop.org/0295-5075/109/i=2/a=26002

[28] J. Bartram and R. Ballance, *Water quality monitoring: a practical guide to the design and implementation of freshwater quality studies and monitoring programmes*. CRC Press, 1996.

[29] F. Segura-Quijano, J. Sacristán-Riquelme, J. García-Cantón, M. T. Osés, and A. Baldi, "Towards fully integrated wireless impedimetric sensors," *Sensors*, vol. 10, no. 4, pp. 4071–4082, 2010.

[30] F. Buckley and A. A. Maryott, *Tables of dielectric dispersion data for pure liquids and dilute solutions*. US Dept. of Commerce, National Bureau of Standards, 1958, vol. 589.

[31] A. Jouyban, S. Soltanpour, and H.-K. Chan, "A simple relationship between dielectric constant of mixed solvents with solvent composition and temperature," *International journal of pharmaceutics*, vol. 269, no. 2, pp. 353–360, 2004.

[32] R. Somaraju and J. Trumpf, "Frequency, temperature and salinity variation of the permittivity of seawater," *IEEE Transactions on Antennas and Propagation*, vol. 54, no. 11, pp. 3441–3448, 2006.

[33] A. V. Rukavina, "Hand-held unit for liquid-type recognition, based on interdigital capacitor," *Measurement*, vol. 51, pp. 289–296, 2014.

[34] G. Akerlof, "Dielectric constants of some organic solvent-water mixtures at various temperatures," *Journal of the American Chemical Society*, vol. 54, no. 11, pp. 4125–4139, 1932.

[35] A. P. Sample, D. J. Yeager, P. S. Powledge, A. V. Mamishev, and J. R. Smith, "Design of an RFID-based battery-free programmable sensing platform," *IEEE Transactions on Instrumentation and Measurement*, vol. 57, no. 11, pp. 2608–2615, 2008.

[36] Z. Qi, Y. Zhuang, X. Li, W. Liu, Y. Du, and B. Wang, "Full passive UHF RFID tag with an ultra-low power, small area, high resolution temperature sensor suitable for environment monitoring," *Microelectronics Journal*, vol. 45, no. 1, pp. 126–131, 2014.

[37] K.-P. Latti, M. Kettunen, J.-P. Strom, and P. Silventoinen, "A review of microstrip t-resonator method in determining the dielectric properties of printed circuit board materials," *IEEE Transactions on Instrumentation and Measurement*, vol. 56, no. 5, pp. 1845–1850, 2007.

[38] N. K. Das, S. M. Voda, and D. M. Pozar, "Two methods for the measurement of substrate dielectric constant," *IEEE Transactions on Microwave Theory and Techniques*, vol. 35, no. 7, pp. 636–642, 1987.

[39] G. Shaker, S. Safavi-Naeini, N. Sangary, and M. M. Tentzeris, "Inkjet printing of ultrawideband (UWB) antennas on paper-based substrates," *IEEE Antennas and Wireless Propagation Letters*, vol. 10, pp. 111–114, 2011.

Wenjing Su (S'14) was born in Hunan, China, in 1991. She received the B.S. degree in electrical engineering from Beijing Institute of Technology, Beijing, China, in 2013 and M.S. degree in electrical and computer engineering from Georgia Institute of Technology, Atlanta, GA, USA, in 2015. She is currently working toward the Ph.D. degree in electrical and computer engineering at Georgia Institute of Technology.

In fall 2013, she joined the Agile Technologies for High-performance Electromagnetic Novel Applications (ATHENA) group as a graduate research assistant. Her research interests are additively manufactured (inkjet/3D-printed) electronics and flexible/wearable RF solutions, such as microfluidics sensors for Internet of Things (IoT) and Lab-on-Chip (LoC) applications, and mechanical/liquid-based tunable antennas as well as passive RF components for wideband/multi-functional reconfigurable communication systems. Her research in ATHENA interfaces the microwave with material science and mechanical engineering to provide novel and low-cost solutions to RF/microwave systems.

Ms. Su was awarded Honors Class Program Scholarship and People's Scholarship for undergraduate study from 2009 to 2013; the IEEE International Microwave Symposium (IMS) PhD Student Sponsorship Initiative in 2014; iREDEFINE professional development award in 2017. Ms. Su is a member of the IEEE Microwave Theory and Techniques Society.

Manos M. Tentzeris (S'89-M'92-SM'03-F'10) received the Diploma degree (magna cum laude) in electrical and computer engineering from the National Technical University of Athens, Athens, Greece and the M.S. and Ph.D. degrees in electrical engineering and computer science from the University of Michigan, Ann Arbor, MI, USA.

He is currently Ken Byers Professor in Flexible Electronics with School of ECE, Georgia Tech, Atlanta, GA. He has published more than 650 papers, 5 books and 25 book chapters, while owing 14 patents and heading the ATHENA research group (20 researchers).

Dr. Tentzeris has been the recipient/co-recipient of numerous awards including the 2017 Georgia Tech Outstanding Achievement in Research Program Development Award, 2016 Bell Labs Award Competition 3rd Prize, the 2015 and 2013 IET Microwaves, Antennas and Propagation Premium Awards, the 2014 Georgia Tech ECE Distinguished Faculty Achievement Award, the 2010 IEEE APS Piergiorgio L. E. Uslenghi Letters Prize Paper Award, the 2009 E.T.S.Walton Award from the Irish Science Foundation, the 2003 NASA Godfrey "Art" Anzic Collaborative Distinguished Publication Award. He was the TPC Chair for IEEE IMS 2008 Symposium. He has been a Visiting Professor with the Technical University of Munich, Germany, with GTRI-Ireland in Athlone, Ireland and with LAAS-CNRS in Toulouse. He has given more than 100 invited talks and is a Fellow of IEEE and a Fellow of the Electromagnetic Academy. Prof. Tentzeris served as one of the IEEE MTT-S Distinguished Microwave Lecturers from 2010-2012 and he is one of the IEEE CRFID Distinguished Lecturers.